Advanced Calculation of the Room-Temperature Shapes of Unsymmetric Laminates

M. SCHLECHT AND K. SCHULTE*
Technical University Hamburg-Harburg
Polymer/Composites Section
21071 Hamburg, Germany

(Received April 10, 1997)
(Revised June 30, 1998)

ABSTRACT: It is well known that the room-temperature shapes of unsymmetric laminates do not always conform to the predictions of classical lamination theory. Instead of being saddle shaped, as classical lamination theory predicts, the room-temperature shapes of unsymmetrically laminated composites are often cylindrical in nature. In addition, a second cylindrical shape can sometimes be obtained from the first by a simple snap-through action. Since 1981 several models, which are restricted to rectangular plates and sometimes only some special lay-ups, have been developed. The Finite Element Analysis (FEA) has just recently been used for the calculation of the room-temperature shapes of unsymmetric laminates, because more sophisticated finite element codes are now available and the calculations can be made in an acceptable time. Using the FEA there are no restrictions concerning the laminate geometry or the lay-up and the snap-through effect can be modeled. Additionally the edge-effects can also be monitored in the FEA results. Unsymmetric laminates can become important for aircraft applications especially for the aeroelastic tailoring.

1. INTRODUCTION

THE ROOM-TEMPERATURE SHAPES of unsymmetric laminates are a result of residual thermal stresses. Residual thermal stresses (RTS) are induced in composite laminates due to the anisotropic expansion properties of the constituents. During manufacturing, laminates are subjected to curing stresses. Because of the thermal expansion mismatch between plies with different fiber orientation, the

*Author to whom correspondence should be addressed at Baker Hughes INTEQ, 2001 Rankin Rd., Houston, TX, P.O. Box 670968, Houston, TX 77267-0968.

0021-9983/99/16 1472–19 $10.00/0

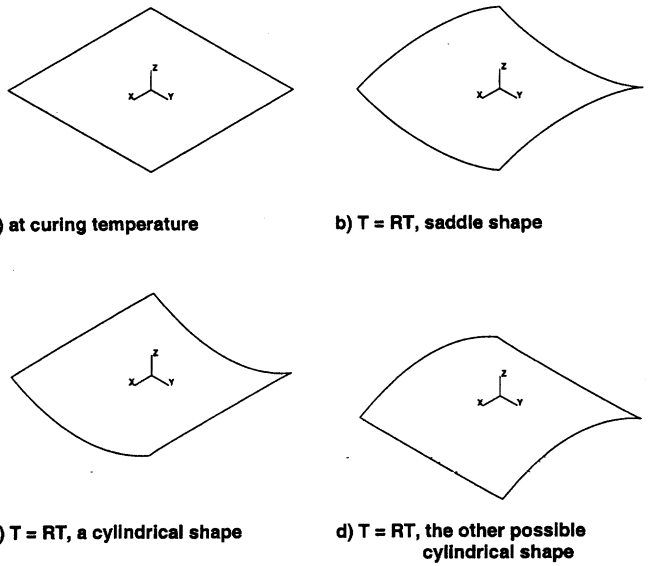

Figure 1. *Laminate shapes: (a) at the elevated curing temperature. At room-temperature, (b) saddle shape, (c) cylindrical shape, (d) the other cylindrical shape.*

RTS manifest themselves in warping unsymmetric laminates. The cured shapes of thin unsymmetric laminates do not conform to the predictions of classical lamination theory (CLT), as had been reported by many investigators [1–8]. Rather than being saddle shaped, as predicted by classical lamination theory, thin unsymmetric laminates are cylindrical-shaped or even exhibit a snap-through phenomenon with two room-temperature shapes (Figure 1). Hyer conducted a series of experiments with several laminate lay-ups and developed a theory for the calculation of $[0_2/90_2]$ and $[0_4/90_4]$ laminates [2–5].

With the extended classical lamination theory it was possible to predict the shapes of the class of all square unsymmetric cross-ply laminates which can be fabricated from four layers, i.e., [0/0/0/90], [0/0/90/0], [0/90/0/90], [0/0/90/90] laminates. Hyer's main idea was to assume that the out-of-plane displacements can be approximated with the equation

$$w(x, y) = \frac{1}{2}(ax^2 + by^2) \tag{1}$$

a and b being constants. The algorithm associated with this family of laminates is

simpler than the one associated with other families, because some of the A_{ij}, B_{ij} and D_{ij} terms are zero in this family. The state of minimal total potential energy is the criterion for a stable shape. Newer theories for the calculation of the cured shapes of unsymmetric laminates with arbitrary lay-up angles make similar assumptions. They are all restricted to rectangular plates. Edge-effects cannot occur because the constants (curvature), which correspond to a and b in Hyer's theory are independent of x and y. The accuracy of the calculated curvature depends always on the order of the approach used. The snap-through effect cannot be simulated.

To generalize the calculations, the Finite Element Analysis was chosen. Well chosen boundary conditions should lead to good results independent of the laminate lay-up. But the finite element code has to be able to deal with temperature dependent material properties, with the nonlinearities occurring, and the problem of multiple solutions. With the finite element code MARC, good results could be achieved in a very short time. The first calculations showed that the whole simulation is very sensitive to the material data used, the temperature steps for cooling down, and the number of layers in the model. The final results are used to compare the calculated geometries and to prove that the FEA model is suitable to calculate the room-temperature shapes of different classes of laminates.

2. MATERIAL PROPERTIES

For the investigations BASF Rigidite® 5250-2/M40B-6k-50B prepregs were used. The NARMCO resin system 5250-2 is a 177°C to 204°C curing bismaleinimid resin with a service temperature range between −59°C and 204°C. The TORAY M40B-6k-50B carbon fibers are high modulus fibers (HM, $E = 392$ GPa). The laminates were cured in a laboratory hot press. All laminates were cooled down below 50°C while holding pressure. The recommended standard postcure has not been carried-out.

2.1 Thermal Properties

The temperature dependent thermal expansion coefficients were determined by the use of *D*igital *S*peckle *P*attern *I*nterferometry (DSPI) [9]. The results of the measurements are shown in Figure 2. The two test specimens used were cut out of laminates that have been produced in separate curing cycles. At least three measurements were taken for each temperature interval.

The values for the thermal expansion coefficients in fiber direction (α_0) were calculated from the values measured for the 25° direction, because they are otherwise too small to be determined directly. There is no linear dependence between temperature and thermal expansion coefficients over the entire temperature range of the curing cycle. In the case of the 0°-lay-up the thermal expansion coefficient slightly increases in the temperature range from 30°C to 120°C and then decreases

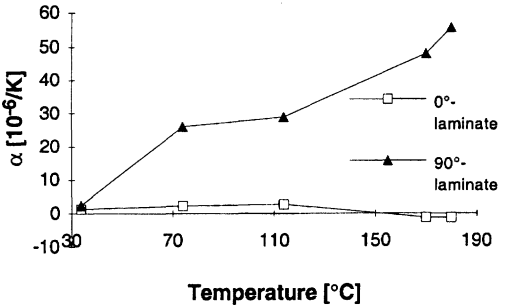

Figure 2. *Temperature dependent thermal expansion coefficients in fiber direction and transverse to the fiber direction.*

and becomes negative. In the case of the 90°-lay-up the thermal expansion coefficient increases relatively fast. Around room-temperature the two thermal expansion coefficients are close together, at elevated temperatures they differ by more than one order of magnitude. These results show that the temperature-dependence of the thermal expansion coefficients has to be considered. For the calculations the extended CLT constant values are used ($\alpha_1 = 2.2 \times 10^{-6}$/K, $\alpha_2 = 2.6 \times 10^{-5}$/K).

2.2 Mechanical Properties

The elastic mechanical properties were also determined in the temperature range between 20°C and 170°C (Figure 3). The relevant mechanical properties at room-temperature are summarized in Table 1.

For the calculations with the extended CLT the material properties at room-temperature are used. The use of temperature dependent material data is possible but would not really change the basic results. For the FEA-simulations a complete set of temperature dependent material data is used (Table 2).

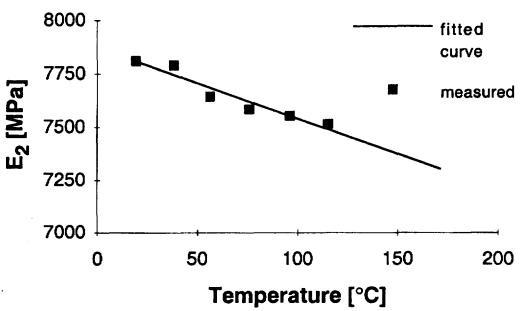

Figure 3. *Transverse modulus (E_2) versus temperature.*

Table 1. Mechanical properties at room-temperature.

E_1 [GPa]	E_2 [GPa]	G_{12} [GPa]	ν_{12}	ν_{21}
252	7.8	6.2	0.32	0.00991

Table 2. Temperature dependent material data

T [°C]	α_{11} [10^{-6}]	α_{22} [10^{-6}]	α_{33} [10^{-6}]	E_{11} [GPa]	E_{22} [GPa]	G_{12} [GPa]	G_{13} [GPa]	G_{23} [GPa]
19.2	—	—	—	252.0	7.81	6.19	6.19	6.19
33.8	1.49	2.39	2.39	—	—	—	—	—
38.2	—	—	—	250.9	7.75	6.02	6.02	6.02
56.2	—	—	—	249.8	7.69	5.85	5.85	5.85
73.8	2.19	26.10	26.10	—	—	—	—	—
75.9	—	—	—	248.5	7.62	5.69	5.69	5.69
96.2	—	—	—	247.3	7.55	5.52	5.52	5.52
113.8	2.72	28.97	28.97	—	—	—	—	—
115.1	—	—	—	246.1	7.49	5.35	5.35	5.35
133.4	—	—	—	245.0	7.43	5.19	5.19	5.19
152.1	—	—	—	243.8	7.37	5.02	5.02	5.02
170.0	−1.25	48.05	48.05	—	—	—	—	—
171.5	—	—	—	242.7	7.30	4.85	4.85	4.85
180.0	−1.26	55.70	55.70	—	—	—	—	—

3. CALCULATION OF ROOM-TEMPERATURE SHAPES

The calculations of the room-temperature shapes were performed with the extended CLT and the FEA for laminates with 0°- and 90°-layers. The FEA was also used to calculate the shapes with arbitrary lay-up-angles and also for a circular laminate. The shape of several laminates was measured and compared with the calculated results.

3.1 Simulation with Finite Element Methods

For the simulation of the warping of the composite laminates the FEA-program MARC (K6.2) was used. This program is able to calculate the behavior of laminated structures with anisotropic and temperature dependent properties and can deal with geometric nonlinearities.

The model has the same size as the manufactured laminates (140 x 140 mm^2). The whole mesh exists of 196 8-node bilinear thick-shell elements (Figure 4). This element allows the calculation of the two normal stresses and the three shear stresses. The laminate lay-up is defined with the integrated Composite option. Each element has a size of 10 × 10 mm^2. For each layer of the real laminate usually two layers are used in the model to increase the accuracy of the results. At the center node all degrees of freedom are fixed. The laminate is usually cooled down from 177°C (curing temperature) to 157°C in steps of 2°C followed by steps of 5°C down to 20°C (room temperature).

An updated Lagrange approach is used to take the geometric nonlinearities into account. In each increment the Newton-Rhapson method is used for the iterations. The convergence testing is based on strain energy, because this is an energetic problem. Additionally the strain energy is a global criterion. The use of residuals or displacements for convergence testing usually only leads to the sad-

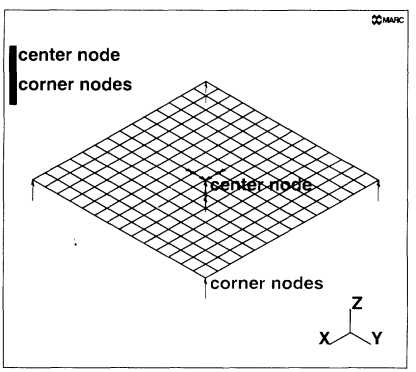

Figure 4. *FEA mesh and boundary conditions.*

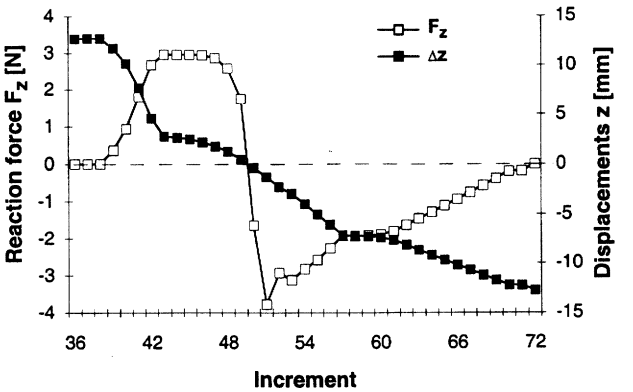

Figure 5. *Displacement of the corner nodes and reaction forces at the center node during simulation of the snap-through of a $[0_2/90_2]$-laminate.*

dle shape and not to cylindrical shapes. The residual loads are corrected, such that the solution is always in equilibrium. For this correction the stresses at all integration points have to be stored. The solution of non-positive definite systems is forced.

For the simulation of the snap-through effect first one room-temperature shape is calculated. Then the four corner nodes are moved in the direction of the supposed second shape (Figure 5, $[0_2/90_2]$-laminate). The calculated reaction force at the center node is positive and increases (increment 38 to 43). Before the snap-through action takes place the reaction force decreases (increment 44 to 49) and becomes negative after the snap-through action (increment 50). After the snap-through the boundary conditions were changed to the old configuration (increment 51 to 72). This is to prove whether the second shape is stable or not.

3.2 Simulation with Extended Classical Lamination Theory

Because Hyer's theory is well documented in the literature [2–5], only some of his basic ideas will be presented in this paper. The classical lamination theory predicts the room-temperature shapes of all unsymmetric laminates to be a saddle with unique curvature characteristics. So this theory is unable to predict the shapes of thin unsymmetric laminates. To explain the behavior of unsymmetric laminates, it was assumed that it would be necessary to incorporate a nonlinear effect into the classical lamination theory. The existence of two room-temperature shapes (i.e., the two cylinders) essentially ruled out a linear extension to the theory, since a linear extension would lead to the prediction of a unique shape, although perhaps not a saddle. Furthermore, since the out-of-plane deflections of the

unsymmetric laminates were in the order of many laminate thicknesses, geometric nonlinearities were felt to be an important effect. So the classical lamination theory was extended to include geometric nonlinearities through the strain-displacement relationship. Possible shapes are those with a minimum of the total potential energy, which leads to multiple solutions of this nonlinear problem. Thus, for stable equilibrium the second variation of the total potential energy, $\delta^2 W$, must be positive definite.

3.3 Results

The aim of this investigation was to determine whether the FEA is able to predict the room-temperature shapes of thin unsymmetric laminates and what are the differences compared to the results of the extended CLT.

First of all, there are some obvious differences. The calculations with the extended CLT can be performed with "Mathematica" on an Apple Macintosh Quadra in a few minutes. As a result you get all possible shapes, and the information whether the calculated shapes are stable or not. A variation of the material properties in a certain range only leads to a variation of the calculated curvatures but usually not to a change of the predicted stable shapes. To perform the simulation with the FEA you need several hours, even on a powerful workstation. As a result you only get one possible stable shape. For the calculation of a second stable shape the snap-through has to be simulated. Slight changes of the material properties can lead to the calculation of a saddle shape instead of a cylindrical shape, especially if the material data are not completely consistent. On the other hand, all stresses, strains and reaction forces are available without any additional effort. One gets more information about the laminate. Up to now it seems that the extended CLT is easier to use and causes less problems. The FEA takes much more time but one gets more information about the laminate. Therefore the results are compared for some laminates, to show the basic differences. A wide variety of laminates was analyzed during these studies. Only the most important results are presented.

3.3.1. $[0_2/90_2]$-Laminate

The Figure 6 shows the results for a $[0_2/90_2]$-laminate: a) calculated with FEA, b) calculated with the extended CLT and c) measured. There is only a slight difference in the maximum displacements in z-direction. A change in the material properties used for the extended CLT could easily lead to the same displacements. The shape calculated with the extended CLT shows no edge effects. Only a unique curvature in one direction can be seen. The curvature in the second direction can be neglected. The edge with no major curvature seems to be straight. The shape calculated with FEA shows a clear edge effect like the measured shape. The edge with the smaller curvature is not straight. It has a slight saddle shape. The dis-

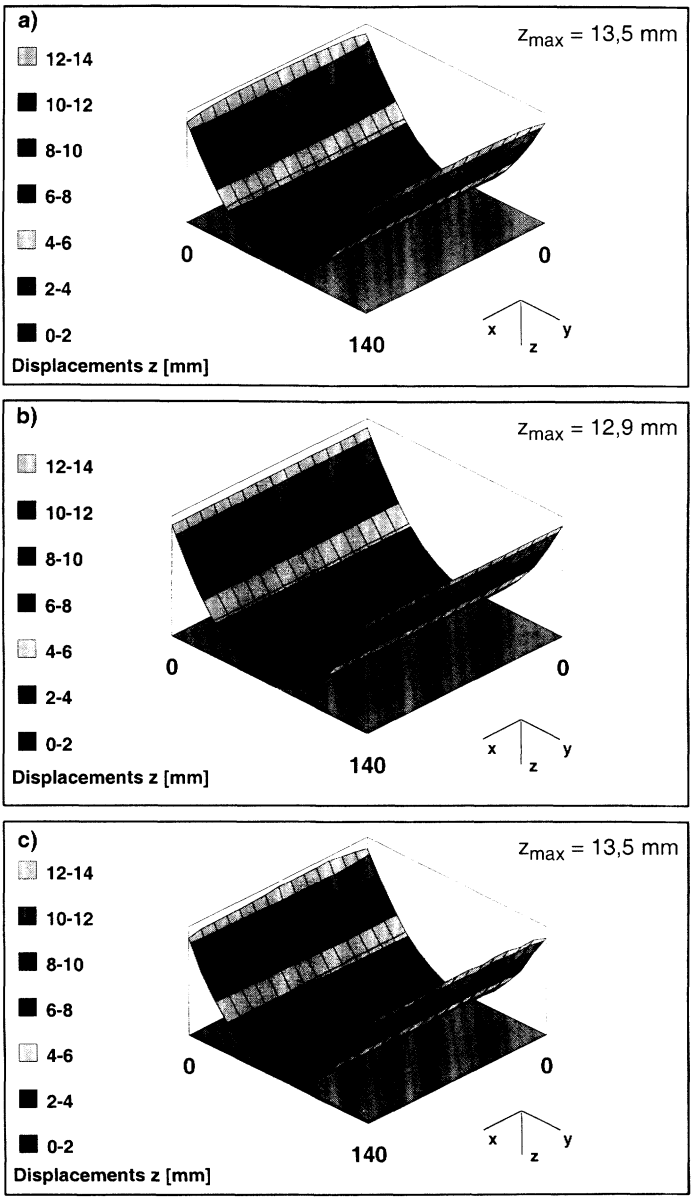

Figure 6. *Deformation of a $[0_2/90_2]$-laminate: (a) calculated with FEA, (b) calculated with the extended CLT and (c) measured geometry.*

placement in z-direction in the corners is not as high as in the middle of the laminate.

The edge effect can clearly be seen in Figure 7. The edge effects of the extended CLT results are only caused by the displacement function $w(x)$ and have no physical background. Even newer theories which are based on the classical lamination theory are unable to describe the occurring edge effects because they use coefficients (curvatures) a and b (Equation 1), which are independent of x and y. The FEA results show the same edge effects as measured by Peeters et al. [8].

The occurring shapes are dependent on the length to thickness ratio. Thick unsymmetric laminates usually have a saddle shape. The influence of the length to thickness ratio was investigated by changing the laminate thickness in a range from $t = 0.1$ mm to $t = 2.0$ mm in steps of 0.1 mm while keeping the sidelength constant at 140 mm. The extended CLT predicts two stable cylindrical shapes for the $[0_2/90_2]$-laminate with a thickness less than $t = 1.7$ mm and the FEA for a thickness below $t = 1.4$ mm. Both methods calculate nearly the same maximum displacements in z-direction for each thickness. The results also correspond very well with the measured displacements. The manufactured laminates had two stable cylindrical shapes or had no curvature. The thick laminates which should have had saddle shapes delaminated between the 0°- and the 90°-layer in the middle of the laminate. Because of this it would be a good idea to use a failure criterion to predict these delaminations in future works.

The calculations were also performed for a $[0_2/90_2]$-laminate with a sidelength of $l = 280$ mm. The finite element mesh consisted of 784 elements, each of a size of 10 x 10 mm. Because the finite element code always predicted a saddle shape, independent of the step width used in each increment, the four corner nodes were moved $\Delta z = 1$ mm in positive z-direction. After this bending to a slight cylinder, the four corner nodes were fixed in this position and the laminate was cooled down for 10°C. After removing the constraints of the corner nodes the laminate was cooled down to the room-temperature. Due to this small trick it was possible to predict the correct room-temperature shape. This procedure can be used in all cases where a saddle shape is predicted instead of the expected cylindrical shape. The measured maximum displacement in z-direction was $\Delta z_{meas} = 52$ mm and the calculated displacement was $\Delta z_{FEA} = 51.3$ mm (FEA) and $\Delta z_{ext\,CLT} = 51.8$ mm (extended CLT). The snap-through effect could also be simulated for this laminate. Due to the model size it takes several hours to perform these calculations on a HP 712/100 Workstation.

3.3.2. Other Laminates with 0°- and 90°-Layers

The $[0/90_3]$-laminate has one stable cylindrical shape as predicted from the FEA and the extended CLT. The calculated maximum displacements are $\Delta z_{max\text{-}ext.\ CLT} = 34.8$ mm (extended CLT) and $\Delta z_{max\text{-}FEA} = 33.6$ mm (FEA), re-

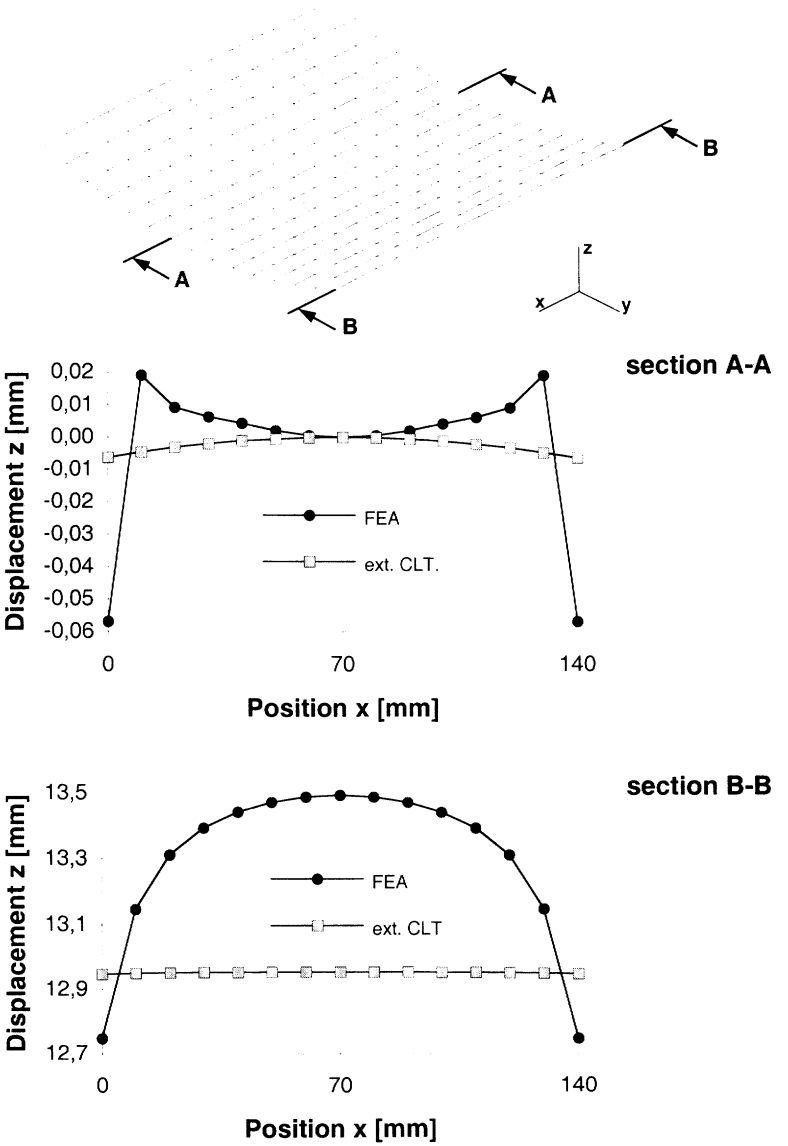

Figure 7. *Edge effect of a $[0_2/90_2]$-laminate, calculated with the extended CLT and FEA: (a) deformed mesh, (b) displacement z at section A-A and (c) displacement z at section B-B.*

spectively. The measured maximum displacement was $\Delta z_{max\text{-}meas} = 35.9$ mm and corresponds very well with the calculations. The calculated shapes are quite similar. The FEA results again show a clear edge effect.

The calculations were also performed for a $[0/90_3]$-laminate with a sidelength of $l = 260$ mm. Due to the extreme deformation a lot of matrix cracks were formed in the 90°-layers. This is a hint, that for proper results for extreme unsymmetric laminates a failure criterion should be incorporated into the model. The extended CLT predicts greater displacements in z-direction and smaller displacements in x-direction than the measured values (Figure 8). With the FEA it was not possible to calculate the room-temperature shape of this laminate. The calculation always aborted at a temperature between $T = 80$°C and $T = 95$°C because the equation system was not positive definite. In this temperature range the edge elements are distorted for nearly 90° and the distance in x-direction between the corner-nodes of each edge-element is nearly zero. Displacements in x-direction of the local coordinate system become z-displacements in the global coordinate system. The used FEA code is not able to handle this problem. Even a rezoning of the mesh failed.

For the $[0_2/90_3]$-laminate the FEA and the extended CLT both predict two stable shapes. The maximum calculated displacements in z-direction for one cylindrical shape are $\Delta z_{max\text{-}ext.\ CLT} = 15.5$ mm (extended CLT) respectively $\Delta z_{max\text{-}FEA} = 16.0$ mm (FEA), whereas the measured displacement is $\Delta z_{max\text{-}meas} = 16.0$ mm. The manufactured laminate only has one stable cylindrical shape. Before getting a second shape the laminate would crack. The second shape predicted from extended CLT is cylindrical with a maximum displacement in z-direction of -4 mm. But this second shape is only predicted below a temperature of 113°C. At higher temperatures only one stable shape is predicted. The second shape predicted with the

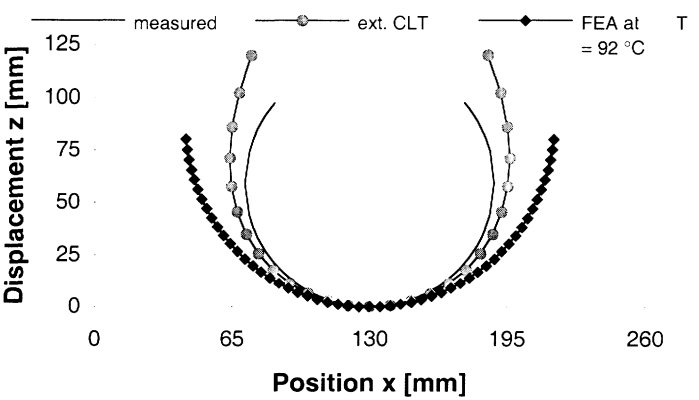

***Figure 8**. Measured and calculated cross-section of a $[0/90_3]$-laminate with a sidelength of l = 260 mm. With the FEA the laminate could only be cooled down to a temperature of T = 90°C. At lower temperatures the equation system is not positive definite and cannot be solved.*

FEA is a saddle shape with different curvatures in the two main directions. The forces needed to snap the laminate into this second shape are nearly three times as high as the forces needed to snap the $[0_2/90_2]$-laminate. Although both calculation methods predict two stable shapes, there is a hint that the second predicted shape is not as stable as the first one or that the second might be impossible.

3.3.3. $[0_2/\phi_2]$-Laminates

In general, square laminates with a $[0_2/\phi_2]$-lay-up exhibit two stable cylindrical shapes or a saddle shape, when the thickness is not small compared to the sidelength. For these laminates the influence of the angle ϕ on the curvature and the forces needed to activate the snap-through action was investigated. The room-temperature shape of the following laminates were calculated and measured:

$$[0_2/15_2] \quad [0_2/30_2] \quad [0_2/45_2] \quad [0_2/60_2] \quad [0_2/75_2]$$

The main curvatures of these laminates are not in the x- and y-direction (Figure 9). For the first cylindrical shape the angle between the direction of the curvature and the x-axes covers a range from $\varphi = 30°$ to $\varphi = 90°$, while the second shapes only cover a range from $\varphi = -25°$ to $\varphi = 0°$ (Figure 10). There is only a slight difference between the measured angles and the calculated angles. The maximum displacements in z-direction occur for the $[0_2/45_2]$-laminate (Figure 11) which corresponds with the measured values. The forces needed to activate the snap-through action increase with an increasing angle ϕ (Figure 12).

3.3.4. Laminates with Other Lay-Ups

Additional calculations have been performed for following laminates:

$$[0/-45/90/+45] \quad [0/-30/90/+30] \quad [0/90_2/60]$$

The $[0/-45/90/+45]$-laminate has two stable cylindrical shapes, while the $[0/-30/90/+30]$ and the $[0/90_2/60]$ only have one stable cylindrical shape. For each real layer of the laminate three layers were used in the model, because these laminates exhibit very high deformations (Figure 13). The main results of the calculation and the measurements are summarized in Table 3. The maximum displacements in x- and y-direction are those of the corner nodes with the highest displacements in z-direction. The calculated curvatures are smaller than the measured ones. But two important aspects have to be taken into account:

1. The measurements were only performed for one laminate. Slight differences of the lay-up angle and in moisture content can change the results.
2. The occurring geometric nonlinearities are very big. The maximum displacements of the $[0/90_2/60]$-laminate are nearly 120 times the laminate thickness.

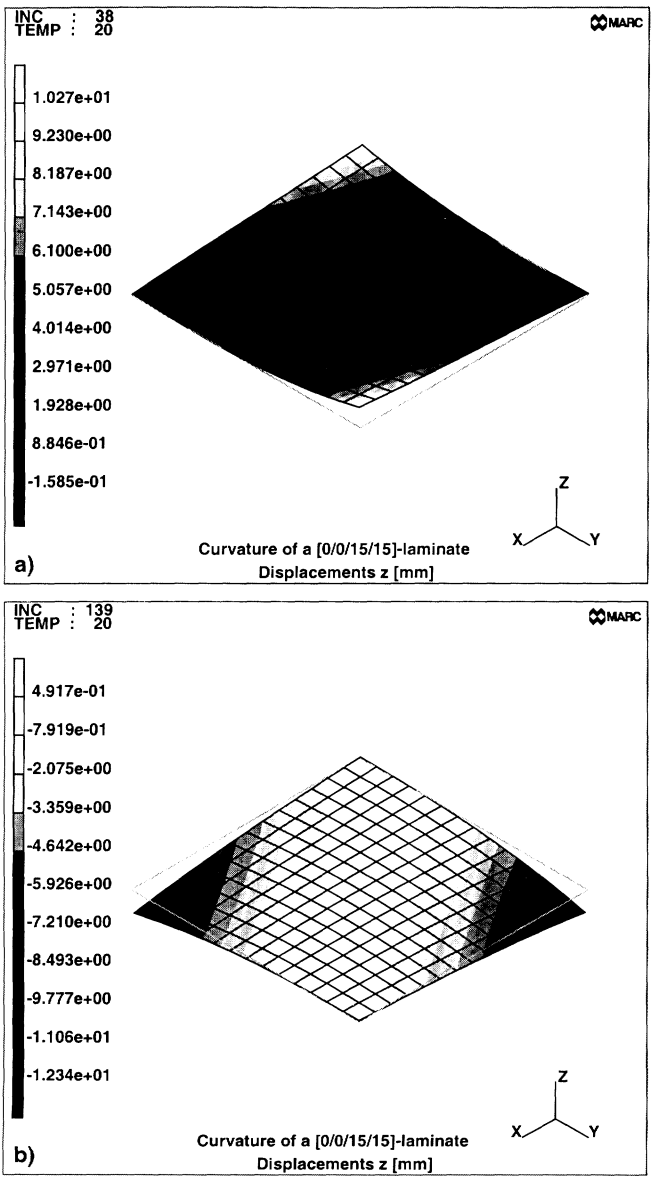

Figure 9. *Room-temperature shapes of a $[0_2/15_2]$-laminate: (a) shape after cooling the laminate down to room-temperature and (b) shape after the simulated snap-through.*

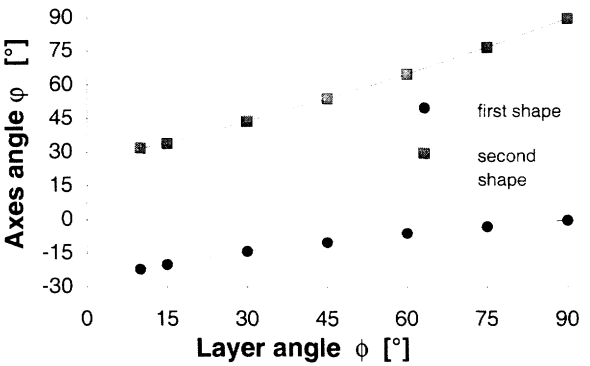

Figure 10. *Calculated direction of curvature versus layer angle ϕ of a $[0_2/\phi_2]$-laminate.*

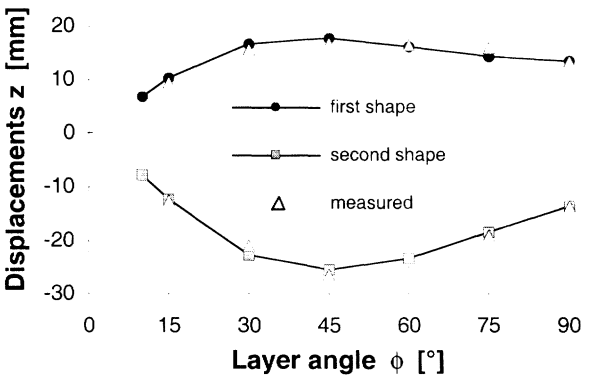

Figure 11. *Calculated displacements z versus layer angle ϕ of a $[0_2/\phi_2]$-laminate.*

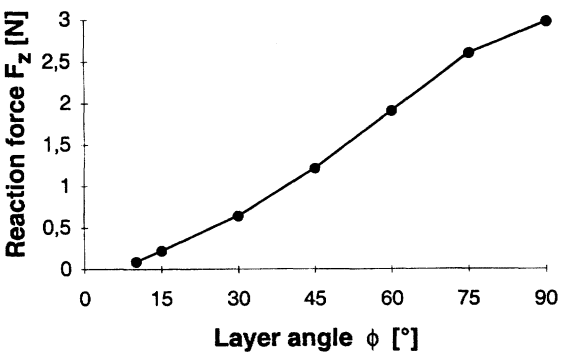

Figure 12. *Maximum reaction forces to snap the laminates versus layer angle ϕ of a $[0_2/\phi_2]$-laminate.*

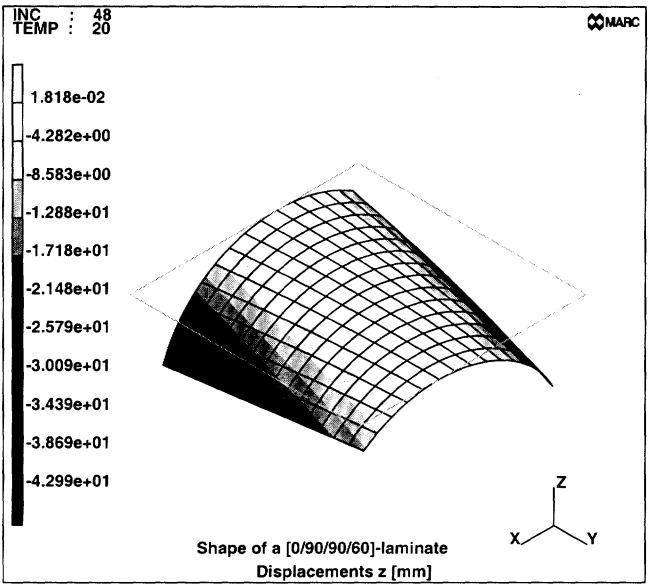

Figure 13. *Room-temperature shape of a [0/90$_2$/60]-laminate.*

3.3.5. Circular Laminate

The main disadvantages of the existing models to calculate the room-temperature shapes of unsymmetric laminates was their restriction to rectangular plates. The FEA is able to handle any geometry. This was proven by the calculation of the room-temperature shape of a circular [0$_2$/90$_2$]-laminate with a diameter of $d = 140$ mm. For the calculations a complete new FEA mesh had to be generated. The resulting stresses show a different distribution. The used mesh has quadratic elements in the center region. The other elements are arranged radially and form the circle. At the center node all degrees of freedom are fixed. The calculations always predicted a saddle shape for this laminate, so that a slight cylindrical

Table 3. Measured and calculated maximum displacements and axes angles ϕ.

Laminate	Δx_{meas} [mm]	Δx_{FEA} [mm]	Δy_{meas} [mm]	Δy_{FEA} [mm]	Δz_{meas} [mm]	Δz_{FEA} [mm]	φ_{meas} [°]	φ_{FEA} [°]
[0/−45/90/+45]	2.0	0.7	3.1	3.0	−18.0	−19.2	−10	−10
[0/−45/90/+45]	3.8	4.1	3.2	2.7	24.5	26.1	55	55
[0/−30/90/+30]	2.4	1.2	9.2	6.1	28.0	26.5	−10	−10
[0/90$_2$/60]	18.6	15.8	7.1	4.6	−43.9	−43.0	75	74

shape had to be forced by moving the nodes marked 1 to 4 into the direction of the first cylindrical shape (Figure 14). These four nodes were also used to snap the laminate to the second shape. The model is built up of 12 layers.

To calculate the first cylindrical shape, nodes 3 and 4 were fixed in z-direction while nodes 1 and 2 were moved for $\Delta z = 1$ mm in z-direction and fixed in this position. After cooling the laminate down to a temperature of $T = 167°C$ in steps of $\Delta T = 0.5°C$, nodes 1 and 2 were released. Nodes 3 and 4 were released after cooling the laminate down to a temperature of $T = 157°C$. During the following cooling down to room-temperature no additional boundary conditions were used. These calculations were also performed for a $[0/90_2/60]$-laminate. For this laminate the cylindrical shape was directly predicted without the use of any additional boundary condition. This is a hint that the problems with the $[0_2/90_2]$-laminate are a result of the used lay-up.

The calculated curvature of the $[0_2/90_2]$-laminate is nearly identical with the measured one. The maximum calculated displacements in z-direction was $\Delta z_{max\ FEA} = 13.9$ mm and the maximum measured displacement was $\Delta z_{max\ meas} = 14.7$ mm, which is only a slight difference.

The snap-through action was performed in several steps. First, nodes 3 and 4 were fixed in z-direction while nodes 1 and 2 were moved in negative z-direction, until all nodes were nearly in the x-y-plane. Nodes 1 and 2 were fixed in this position, while nodes 3 and 4 were moved for $\Delta z = 4$ mm in negative z-direction. In

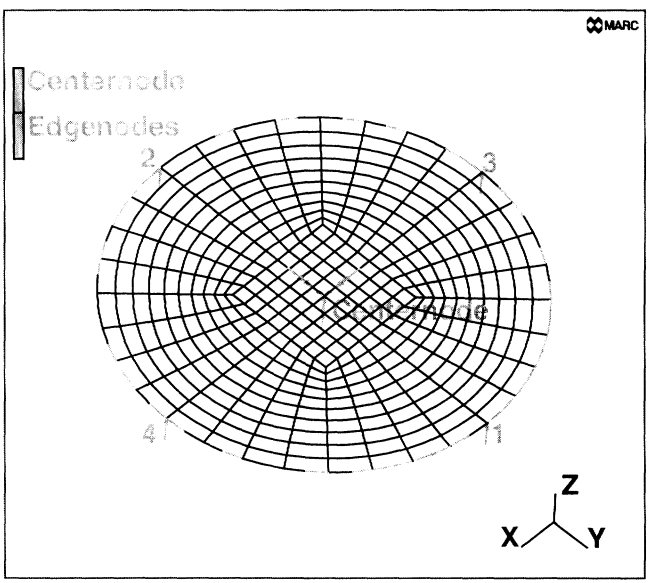

Figure 14. *FEA mesh and boundary conditions.*

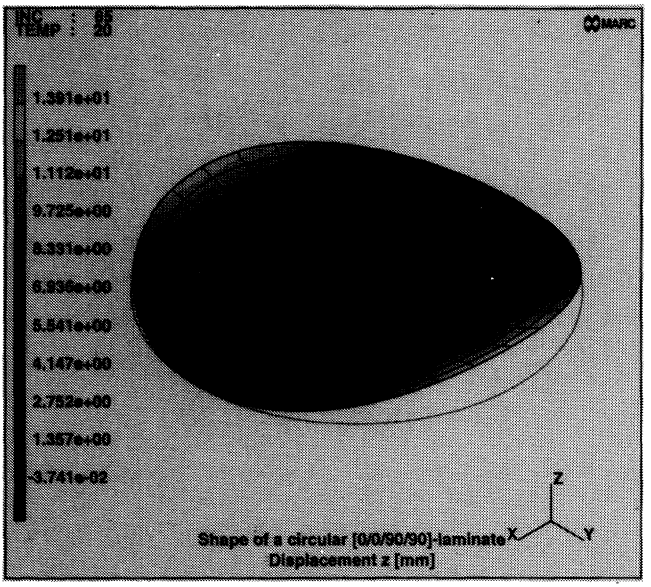

Figure 15. *Room-temperature shape of a circular [0_2/90_2]-laminate.*

this position nodes 1 and 2 were released. Finally nodes 3 and 4 were moved completely to the second cylindrical shape, where they also were released. The second calculated shape was the same as the first one.

4. CONCLUSION

The FEA as well as the extended CLT are able to predict the room-temperature shapes of thin unsymmetric laminates. The results have been proven experimentally. Hyer extensively calculated the size influence on the reported effect. The calculations with the FEA were performed for different laminate sizes, shapes and for different lay-ups with arbitrary lay-up angles. All results demonstrate that the FEA is a well suited tool to calculate the room-temperature shapes of different classes of laminates with different shapes. The whole snap-through action can be simulated. Some results give the hint that a failure criterion should be integrated into the laminate. The major difference between the results from both methods are the displacements in z-direction calculated for the edges. The manufactured laminates show the same edge effects as the FEA results. In addition more information about the internal stresses and forces needed to initiate a snap-through action are raised, with the only drawback, that a powerful workstation is needed and more time to perform the calculations. With the FEA the room-temperature shapes of any unsymmetric laminate can be calculated and by this

means it is a good tool for developments, e.g., in the fields of aeroelastic tailoring or smart structures.

ACKNOWLEDGMENTS

The authors acknowledge the assistance of Frau Dr.-Ing P. Aswendt (Fraunhofer Einrichtung für Umformtechnik und Werkzeugmaschinen, Chemnitz, Germany) for determining the thermal expansion coefficients and the Deutscher Akademischer Austauschdienst (DAAD) for partly funding this work. The measurements of the room-temperature shapes of several laminates were performed at BMW AG, Munich.

REFERENCES

1. M. Schlecht, K. Schulte, M. W. Hyer: "Advanced calculation of the room-temperature shapes of thin unsymmetric composite laminates," Composite Structures, Vol. 32, 1995, 627–633.
2. Hyer, M. W.: The room-temperature shapes of four-layer unsymmetric cross-ply laminates. Journal of Composite Materials, Vol. 16, 1982, 318–340.
3. Hyer, M. W.: Unsymmetrically laminated composites. Proc. of the 4th International Conference on Composite Materials (ICCM-IV), ed. T. Hayashi, K. Kawata, S. Umekawa, Tokyo, 1982, 373–380.
4. Hyer, M. W.: Some observations on the cured shapes of thin unsymmetric laminates. Journal of Composite Materials, Vol. 15, 1981, 175–194.
5. Hyer, M. W.: Calculations of the room-temperature shapes of unsymmetric laminates. Journal of Composite Materials, Vol. 15, 1981, 296–320.
6. Hahn, H. T.: Warping of unsymmetric crossply graphite/epoxy laminates. Composites Technology Review, Vol. 3, 1981, 114–117.
7. Jun, W. J., Hong, C. S.: Cured shapes of unsymmetric laminates with arbitrary lay-up angles. Journal of Reinforced Plastics and Composites, Vol. 11, 1992, 1352–1366.
8. Peeters, L. J. B., Powell, P. C., Warnet, L.: Thermally-induced shapes of unsymmetric laminates. Journal of Composite Materials, Vol. 30, No. 5, 1996, 603–626.
9. Aswendt, P., Höfling, R.: Speckle interferometry for analysing anisotropic thermal expansion—application to specimens and components. Composites, Vol. 24, 1993, 611–617.